Sum of all Black-Scholes-Merton models: An efficient pricing method for spread, basket, and Asian options

Jaehyuk Choi

Peking University HSBC Business School, University Town, Nanshan District, Shenzhen 518055, China

jaehyuk@phbs.pku.edu.cn

This study considers pricing multi-asset options under Black-Scholes-Merton (BSM) models, such as basket, spread, and Asian options. Contrary to the common view that exact pricing is computationally prohibitive due to the curse of dimensionality, we present an efficient pricing method which quickly converges to the true option value. We express the option price as a quadrature integration over the analytic multi-asset BSM prices under a single Brownian motion. The key to this approach is to rotate the state space in favor of the numerical integration, so that the quadrature requires much coarser nodes than it otherwise would or low varying dimensions can be reduced. We thereby generalize the BSM model into a multi-asset framework by replicating the value of the option on a linear combination of assets as a weighted sum of a parsimonious set of single-factor BSM prices. The accuracy and efficiency of our method is illustrated by various numerical experiments.

Key words: multi-asset Black-Scholes-Merton, spread option, basket option, Asian option, curse of dimensionality

1. Introduction

1.1. Background

Ever since the celebrated success of the Black-Scholes-Merton (BSM) model, the effort to extend its simple analytic solution to the derivatives written on multiple underlying assets has long been of great interest to researchers (Broadie and Detemple 2004). One important class of such derivatives is that of the options on a linear combination of the assets following correlated geometric Brownian motions (GBMs), which includes the following three popular option types:

- Spread option: European-style option on the difference of two asset prices.
- Basket option: European-style option on the sum of multiple asset prices with positive weights.
- Asian option: option on the average price of one underlying asset on a pre-determined *discrete* set of times or on a *continuous* time range.

These three option types together are arguably the most actively traded non-vanilla options on exchanges or over-the-counter markets. This is because linear combination is a natural way of associating the multiple prices, either of different assets or at different times, and the options on

1

such can provide customized hedge or risk exposure. For examples and financial motivations, we refer to the introductions of Carmona and Durrleman (2003) and Linetsky (2004).

Yet, the pricing of such options under the BSM model, not to mention the models beyond BSM, is not trivial. This is because, unlike normal random variables (RVs), a linear combination of correlated lognormal RVs does not fall back to the same class of distribution, nor has a distribution expressed by any analytic form in general. Therefore, the exact valuation of the option price involves a multidimensional integral over the positive payoff under the risk neutral measure. The numerical evaluation of such an integral, however, suffers from the curse of dimensionality. For example, even a coarse discretization of a standard normal distribution from -5 to 5 with the grid size 0.25 (41 points per dimension) leads to 3 million points for four assets and 116 million points for five assets, which substantially exceed the size of typical Monte Carlo simulation.

1.2. Literature review

There is a vast amount of literature on each of the three option types. Firstly, we review analytic approximation methods, in which either the option price is approximated or the lower and upper bound of the price is provided. For the spread option, Kirk's formula (Kirk 1995) has been widely used in practice. It is an approximate generalization of Margrabe's formula (Margrabe 1978) for an exchange option, that is, a spread option with a zero strike price, and several improvements to the formula have followed (Bjerksund and Stensland 2014, Lo 2015). Carmona and Durrleman (2003) computes the lower bound of a spread option price as the maximum over the prices from all possible linear, therefore sub-optimal, exercise boundaries. Li et al. (2008) proposes a closed-form formula based on a quadratic approximation of the exercise boundary.

Basket and Asian options share the underlying ideas for analytic approximations because the payoff of an Asian option depends on the basket of the correlated prices over the observation times. Among the most popular approaches is to approximate the distribution of the GBM sum with other analytically known distributions such as lognormal (Levy and Turnbull 1992, Levy 1992), reciprocal gamma (Milevsky and Posner 1998a,b), shifted lognormal (Posner and Milevsky 1998, Borovkova et al. 2007), log-extended-skew-normal (Zhou and Wang 2008), and those with perturbation expansions from known distributions (Turnbull and Wakeman 1991, Ju 2002). Another popular idea is to exploit the geometric, as opposed to the arithmetic, mean of GBMs whose distribution is lognormal and, hence, is analytically solvable. The option price on the geometric mean serves as a reasonable proxy for that on the arithmetic mean (Gentle 1993). Thus, it can be used as a control variate, reducing the Monte Carlo variance for Asian (Kemna and Vorst 1990) and basket options (Krekel et al. 2004). Curran (1994) uses the geometric mean as a conditioning variable to provide an analytic estimation of option prices. The conditioning approach is further refined by

Beisser (1999) and Deelstra et al. (2004), and is also applied to the continuously monitored Asian options (Rogers and Shi 1995). For other pricing approaches for basket and Asian options, as well as their classification, we refer to Zhou and Wang (2008) and the references therein.

The analytic approximation methods are appealing because the computation is simple. However, the major limitation is that the results are not exact. While each method is accurate for certain ranges of parameters where the underlying assumptions are valid, it is rare that one method is accurate for all ranges of the parameters. In basket options, for example, no single method performs well under various parameter sets (Krekel et al. 2004), although that of Ju (2002) is outstanding overall. Therefore, practitioners must carefully identify the comfort range of parameters in which a method of interest works well. Given the multi-asset aspect of the problem, it is not trivial to *chart* the map of parameters in advance. Moreover, the error cannot be controlled within the approximation methods; thus, one eventually resorts to external methods, typically Monte Carlo simulation, to obtain a benchmark value.

Convergent pricing methods are fewer in number than are approximation methods. By *convergent*, we mean that a method can produce a deterministic price, as opposed to that from Monte-Carlo method, and it converges to the true value within a reasonable amount of computation, as computational parameters (e.g., grid size) are tuned. For a spread option, convergent methods are feasible because the problem is only two-dimensional. Ravindran (1993) and Pearson (1995) reduce the price to a one-dimensional integration over the BSM prices with varying spot and strike prices. In addition, Dempster and Hong (2002) and Hurd and Zhou (2010) apply a two-dimensional fast Fourier transform (FFT).

To the best of the author's knowledge, few studies on basket options fit into the definition of the convergent method. In particular, there has been no attempt to use direct integration, even for the purpose of the error measurement, indicating the challenge in the approach (see § 4.1). The FFT approach of Leentvaar and Oosterlee (2008), although it reduces the computation time by parallel partitioning, does not significantly reduce the amount of computation.

The previous convergent methods for Asian options exploit that the pricing concerns a single price process over time. The continuously averaged Asian option, although hardly traded in practice due to its contractual difficulty, has analytic solutions in the form of triple integral (Yor 1992), Laplace transform in maturity (Geman and Yor 1993), and series expansion (Linetsky 2004). For discrete averaging, there has been a series of studies exploiting the recursive convolution, the so-called Carverhill-Clewlow-Hodges factorization, of the probability density function (PDF) or price (Carverhill and Clewlow 1990, Benhamou 2002, Fusai and Meucci 2008, Černỳ and Kyriakou 2011, Fusai et al. 2011, Zhang and Oosterlee 2013). Cai et al. (2013) express the price of a discretely monitored Asian option as an asymptotic expansion on a small observation interval.

Despite the structural similarity, there have been limited studies that can be applicable to all three option types. Carmona and Durrleman (2005) extends the lower bound approach (Carmona and Durrleman 2003) to a multi-asset problem, while Deelstra et al. (2010) make use of the commonality theory to approximate the option price. However, these studies belong to the class of analytic approximation and, therefore, the methods suffer the aforementioned limitations. As such, we believe that there is no convergent method that consistently works for all three types.

1.3. Contribution of paper

This paper aims to provide an efficient and unified pricing method for the options on linear combinations of the correlated GBMs. Contrary to the common assumption that the outright multidimensional integration is computationally prohibitive, we develop an innovative integration scheme in which the curse of dimensionality is significantly alleviated. We, first, observe that if all the price processes are driven by one Brownian motion, the option price is analytically given by a multidimensional extension of the BSM formula, with the exercise boundary obtained from numerical root-finding. Therefore, the integration for the option price can be done analytically for the first dimension and numerically for the rest. The key to our approach is to choose the first dimension via factor rotation in such a way that the analytic price from the first dimension is made best-behaved (i.e., smooth and slowly varying) as an integrand for the numerical integration that follows. Numerical experiments show that even a coarse discretization produces a very accurate price, and the price quickly converges to the true value as the number of nodes are increased.

The contributions of our results in the context of each type are in order. Our approach is similar to those of Ravindran (1993) and Pearson (1995) for spread options, to the extent that the integration in the first dimension is done analytically. However, the factor rotation in our method significantly reduces the cost of the numerical integration in the second dimension. Even at the expense of the extra computation from the numerical root-finding, which is not present in the aforementioned studies, overall computation is made much lighter due to the reduced discretization on the second dimension.

With regard to basket options, we believe that our method serves as a fully convergent method. While the speed of the convergence depends on the covariance structure in general, our method is capable of converging to the true option value for wide ranges of parameters and dimensions. For the first time, we report the converged prices for several benchmark tests used in literature.

For the study of Asian options, our pricing scheme is a novel alternative to the previous works. The integration approach is particularly cursed in Asian option due to the large dimensionality, that is, the number of observations. In effect, our method utilizes the first several factors of a series representation of Brownian motion in a similar way to PCA. As such, our method falls short

of a truly convergent method. Yet, our method is surprisingly accurate for all practical purposes and the computation is cheaper than those of the existing methods. In addition, our method is capable of pricing a continuously monitored Asian option in a discrete monitoring framework, whereas approaches in the opposite direction have been abundant. To this extent, it can flexibly handle the features, such as non-uniform weights, non-uniform averaging intervals (e.g., forward-start averaging), and time-dependent volatility, which are difficult to incorporate into the methods based on continuum theory (Linetsky 2004, Cai et al. 2013, Fusai et al. 2011). More details on Asian options are discussed in § 5.

While this paper focuses on the BSM model, it is potentially useful for other models. The result can be trivially modified to the displaced GBMs as we show a numerical example in §6. The displaced GBMs have an extra degree of freedom to capture the volatility skew, if not full smile, observed in option market. Our result can also be applied to the stochastic volatility models such as Hull and White (1987), Heston (1993) and stochastic-alpha-beta-rho (Hagan et al. 2002). Under those models, the options are priced by conditional Monte-Carlo method where the price is expressed an expectation of the BSM prices conditional on the quantities such as terminal volatility and integrated variance; see Willard (1997), Broadie and Kaya (2006), and Cai et al. (2017) respectively. Thus, the availability of an efficient BSM pricing method is critical for pricing spread or basket options under such approaches. However, the detailed implementation is beyond the scope of this study.

This paper is organized as follows. Section 2 formulates the problem and Section 3 outlines the multidimensional integration scheme. Section 4 discusses the optimal rotation of the dimensions that facilitates the integration. Section 5 discusses some implications for the Asian option. Section 6 reports the numerical results and, finally, Section 7 concludes.

2. Model setup and preliminaries

Assume that the asset prices, S_k for $1 \leq k \leq N$, follow the correlated GBMs under the risk-neutral measure:

$$\frac{dS_k(t)}{S_k(t)} = (r - q_k)\, dt + \sigma_k\, dW_k(t), \tag{1}$$

where σ_k is the volatility, q_k is the dividend rate, r is the risk-free interest rate, and $W_k(t)$ is a standard Brownian motion with the correlation structure $dW_k(t)dW_j(t) = \rho_{kj}dt$ ($\rho_{kk} = 1$). The options we consider are those whose final payoff depends on a linear combination of the asset prices observed earlier than or at expiry T. The payoff of a vanilla call option with the strike price K is as follows:

$$\left(\sum_{k=1}^{N} w_k\, S_k(t_k) - K\right)^+, \tag{2}$$

for the weights, w_k, and observation times, $0 \le t_k \le T$. Here, $(x)^+ = \max(x, 0)$ is the positive-part operator. Our setup is generic enough to include, but not be limited to, the three option types:

- European spread option: $w_k < 0$ for some, but not all, k and $t_k = T$ for all k.

- European basket option: $w_k > 0$ and $t_k = T$ for all k.

- Asian option: $w_k > 0$ for all k with $\sum w_k = 1$ and $0 \le t_1 < \cdots < t_N = T$. The price processes are all identical, $S_k(t) = S_j(t)$ for $k \ne j$; hence, the index k is omitted without ambiguity, for example, $S(t)$, $W(t)$, σ, and q. The continuously monitored Asian option, whose payoff is $(\frac{1}{T}\int_0^T S(t)dt - K)^+$, will be considered in the discrete framework.

Before we proceed further, we set a few notations and conventions. For a matrix $\boldsymbol{A}$, we note the k-th row vector of $\boldsymbol{A}$ by $\boldsymbol{A}_{k*}$, j-th column vector of $\boldsymbol{A}$ by $\boldsymbol{A}_{*j}$, and (k, j) component of $\boldsymbol{A}$ by A_{kj}. Using these notations, for example, a matrix multiplication $\boldsymbol{C} = \boldsymbol{A}\boldsymbol{B}$ can be expressed as $C_{kj} = \boldsymbol{A}_{k*}\boldsymbol{B}_{*j}$. The transpose of $\boldsymbol{A}$ is noted by $\boldsymbol{A}^T$ and the identity matrix by $\boldsymbol{I}$. For a vector $\boldsymbol{x}$, the k-th component is noted by x_k. Moreover, unless otherwise stated, a vector is a column vector. The L^2-norm of $\boldsymbol{x}$ is $|\boldsymbol{x}| = \sqrt{\boldsymbol{x}^T\boldsymbol{x}}$ and the Frobenius norm of $\boldsymbol{A}$ is $\|\boldsymbol{A}\|_F = (\sum_{k,j} A_{kj}^2)^{1/2}$. Further, unless otherwise specified, the dimensions of a matrix are $N \times N$, size of a vector is N, and indices, k and j, run from 1 to N. For the factor matrix $\boldsymbol{V}$ to be defined below, k is used for indexing rows (assets) and j for indexing columns (Brownian motions or factors). Throughout this paper, we use the terms *factor* and *dimension* interchangeably.

Under the BSM model, the log prices, $\log S_k(t_k)$, follow correlated normal distributions, with the covariance matrix $\boldsymbol{\Sigma}$ given as:

$$\Sigma_{kj} = \rho_{kj}\sigma_k\sigma_j \min(t_k, t_j). \tag{3}$$

If we let $\boldsymbol{V}$ equal a square root matrix of $\boldsymbol{\Sigma}$, satisfying $\boldsymbol{V}\boldsymbol{V}^T = \boldsymbol{\Sigma}$, the T-forward value of the observation $S_k(t_k)$ can be decorrelated to:

$$S_k(t_k)e^{r(T-t_k)} \stackrel{d}{=} F_k \exp(-\frac{1}{2}\Sigma_{kk} + \boldsymbol{V}_{k*}\boldsymbol{z}), \tag{4}$$

where $\boldsymbol{z}$ is a vector of independent standard normal RVs and $F_k = S_k(0)\, e^{rT - q_k t_k}$ is the T-forward price observed at $t = 0$. The symbol $\stackrel{d}{=}$ stands for equality in distribution law. Since $\boldsymbol{V}$ is multiplied to the state vector $\boldsymbol{z}$, we refer to it as a risk factor matrix, or simply a factor matrix. The square root matrix $\boldsymbol{V}$ is not unique. Although the Cholesky decomposition $\boldsymbol{C}$ is a popular choice, any matrix rotated from $\boldsymbol{C}$, as $\boldsymbol{V} = \boldsymbol{C}\boldsymbol{Q}$ for an orthonormal matrix $\boldsymbol{Q}$, is also a square root matrix of $\boldsymbol{\Sigma}$. Note, however, that the norm of the row vectors $|\boldsymbol{V}_{k*}|$ is invariant under any rotation, since $|\boldsymbol{V}_{k*}|^2$ is the variance of the k-th asset's return, $|\boldsymbol{V}_{k*}|^2 = \boldsymbol{V}_{k*}\boldsymbol{V}_{*k} = \Sigma_{kk}$. Further, the Frobenius norm of $\boldsymbol{V}$ is also invariant, since $\|\boldsymbol{V}\|_F^2 = \sum_k |\boldsymbol{V}_{k*}|^2 = \sum_k \Sigma_{kk}$.

The forward value of the call option price becomes an N-dimensional integration:

$$C = \int_{\boldsymbol{z}} \Big(\sum_k w_k F_k \exp(-\frac{1}{2}\Sigma_{kk} + \boldsymbol{V}_{k*}\boldsymbol{z}) - K \Big)^+ n(\boldsymbol{z}) \, d\boldsymbol{z}, \tag{5}$$

where $n(\boldsymbol{z})$ is the multivariate standard normal PDF.

3. Integration scheme

3.1. Single-factor Black-Scholes-Merton formula on first dimension

The analytic tractability of the BSM model can be extended to the multi-asset case when all assets are driven by a single Brownian motion. Let us consider the integration over the first dimension z_1 only:

$$C_{\mathrm{BS}}(\dot{\boldsymbol{z}}) = \int_{-\infty}^{\infty} \Big(\sum_k w_k F_k \, f_k(\dot{\boldsymbol{z}}) \exp\big(-\frac{1}{2}V_{k1}^2 + V_{k1}z_1 \big) - K \Big)^+ n(z_1) \, dz_1, \tag{6}$$

where the dependence on the other dimensions is absorbed into the coefficient function defined as:

$$f_k(\dot{\boldsymbol{z}}) = \exp\Big(-\frac{1}{2}\sum_{j=2}^{N} V_{kj}^2 + \boldsymbol{V}_{k*}\dot{\boldsymbol{z}} \Big) \quad \text{for} \quad \dot{\boldsymbol{z}} = (0, z_2, \cdots, z_N)^T. \tag{7}$$

While $\dot{\boldsymbol{z}}$ has $z_1 = 0$ for computational convenience, $F(\dot{\boldsymbol{z}})$ for a function F should be understood as $F(z_2, \cdots, z_N)$. Note that $f_k(\dot{\boldsymbol{z}}) > 0$ and $E(f_k(\dot{\boldsymbol{z}})) = 1$ for all k. The value $C_{\mathrm{BS}}(\dot{\boldsymbol{z}})$ can be seen as the price of an option on the weighted asset prices driven by a single Brownian motion, where the forward price is $F_k f_k(\dot{\boldsymbol{z}})$, and the standard deviation of the log price is V_{k1} for the k-th asset.

This one-dimensional integration can be analytically evaluated only if the region of the positive payoff is identified. In order to find the roots of the payoff, however, we have to resort to a numerical method such as that of Newton-Raphson. For a reason we explain below in § 4.2, we can pick $\boldsymbol{V}$ such that the payoff is monotonically increasing in z_1, and there always exists a unique root, $z_1 = -d(\dot{\boldsymbol{z}})$, of the equation:

$$\sum_k w_k F_k \, f_k(\dot{\boldsymbol{z}}) \exp\big(-\frac{1}{2}V_{k1}^2 + V_{k1}z_1 \big) = K. \tag{8}$$

The integration from $-d(\dot{\boldsymbol{z}})$ to ∞ yields:

$$C_{\mathrm{BS}}(\dot{\boldsymbol{z}}) = \sum_k w_k F_k f_k(\dot{\boldsymbol{z}}) N(d(\dot{\boldsymbol{z}}) + V_{k1}) - K N(d(\dot{\boldsymbol{z}})), \tag{9}$$

which is a multi-asset extension of the BSM formula. The original BSM formula is a special case for the single asset case ($N = 1$, $t_1 = T$, and $w_1 = 1$):

$$C = F_1 \, N(d + V_{11}) - K \, N(d) \quad \text{for} \quad d = \frac{\log(F_1/K)}{V_{11}} - \frac{V_{11}}{2}, \tag{10}$$

where $\boldsymbol{V}$ is a scalar value, $V_{11} = \sqrt{\Sigma_{11}} = \sigma_1 \sqrt{T}$.

Despite the cumbersome numerical root finding, the analytic integration over z_1 plays an important role, more than just the reduction of one dimension in the integration. First, due to the cusp of the option payoff at the strike, numerical integration on the first factor would otherwise require the densest discretization. Thus, the analytic integration allows us to skip the most computationally costly dimension, albeit at the expense of the numerical root-finding. Second, the first dimension has a degree of freedom from the factor matrix rotation; therefore, we can choose $\boldsymbol{V}$ in favor of the numerical integrations to follow (see §4.2). The integration on the first factor is exact and computationally inexpensive, regardless of the choice of $\boldsymbol{V}$, because it is analytic. Lastly, the analytic pricing is capable of capturing the tail probability (e.g., option price of a far-out-of-the-money strike), which Monte Carlo simulation or discretization-based numerical integration cannot easily capture.

3.2. Quadrature integration on other dimensions

The integration over the other dimensions $\dot{\boldsymbol{z}}$ is performed using numerical quadrature. As the integration is weighted by the normal distribution density, Gauss-Hermite quadrature (GHQ) is the most suitable choice. Let $\{\dot{\boldsymbol{z}}_m\}$ and $\{h_m\}$ be the points and weights, respectively, of the GHQ associated with $n(\boldsymbol{z})$, generated over the dimensions $(z_2, \cdots, z_N)$. Then, the option price becomes a weighted sum:

$$C = \int_{\dot{\boldsymbol{z}}} C_{\mathrm{BS}}(\dot{\boldsymbol{z}}) \, n(\dot{\boldsymbol{z}}) \, d\dot{\boldsymbol{z}} = \sum_{m=1}^{M} h_m \, C_{\mathrm{BS}}(\dot{\boldsymbol{z}}_m). \tag{11}$$

Here M is the total number of nodes, $M = \prod_{j=2}^{N} M_j$, where M_j is the node size of the j-th dimension. Therefore, we cast the option price on a linear combination of the asset prices into a weighted sum of the multi-asset BSM prices of (9), where the forward prices of the assets are varied as $F_k \, f_k(\dot{\boldsymbol{z}}_m)$.

Moreover, the same integration scheme can be applied to quantities of interest other than the call option price. A few examples are given below.

- **Price of put option**:

$$P = \sum_{m=1}^{M} h_m \, P_{\mathrm{BS}}(\dot{\boldsymbol{z}}_m) \quad \text{where} \quad P_{\mathrm{BS}}(\dot{\boldsymbol{z}}) = K N(-d(\dot{\boldsymbol{z}})) - \sum_k w_k F_k f_k(\dot{\boldsymbol{z}}) N(-d(\dot{\boldsymbol{z}}) - V_{k1}) \tag{12}$$

- **Price of binary call option**:

$$D = \sum_{m=1}^{M} h_m N(d(\dot{\boldsymbol{z}}_m)) \tag{13}$$

- **Delta of the forward price F_k**:

$$D_k = w_k \sum_{m=1}^{M} h_m f_k(\dot{\boldsymbol{z}}_m) \, N(d(\dot{\boldsymbol{z}}_m) + V_{k1}) \tag{14}$$

3.3. Dimensionality reduction

Since the problem involves the factor matrix $\boldsymbol{V}$, the possibility of dimensionality reduction of the low varying factors in the context of PCA naturally arises. We take the following approach in order to minimize the side effect. Without a loss of generality, let us assume that the strengths of the factors, $|\boldsymbol{V}_{*j}|$, are in decreasing order of j, and that we want to reduce the dimensions for $N' < j \leq N$, because those $|\boldsymbol{V}_{*j}|$ are small. Then, we can assume that the variation of $d(\dot{\boldsymbol{z}})$ on such z_j is also small, so we drop the dependence on those dimensions as $d(\dot{\boldsymbol{z}}) \approx d(\ddot{\boldsymbol{z}})$, where $\ddot{\boldsymbol{z}} = (0, z_2, \cdots, z_{N'}, 0, \cdots)^T$ is the state vector of the surviving dimensions, with zeros padded on the rest for convenience. In addition, the notation $d(\ddot{\boldsymbol{z}})$ should be interpreted as $d(z_2, \cdots, z_{N'})$. Once the dependence of $C_{\mathrm{BS}}(\dot{\boldsymbol{z}})$ on the reduced dimensions is only through $f_k(\dot{\boldsymbol{z}})$, the integration of (11) over the truncated dimensions can be moved to (9) instead, and can be done analytically. With an abuse of notation, the integral of $f_k(\dot{\boldsymbol{z}})$ over those dimensions is similarly given as:

$$f_k(\ddot{\boldsymbol{z}}) = \exp\left(-\frac{1}{2}\sum_{j=2}^{N'} V_{kj}^2 + \boldsymbol{V}_{k*}\ddot{\boldsymbol{z}}\right). \tag{15}$$

This way, the forward price is preserved as $F_k = E(F_k f_k(\ddot{\boldsymbol{z}}))$, even after the dimensionality reduction. The previous results, (8), (9), and (11), remain remarkably consistent under the reduced dimensions with pure notational changes, N to N', $\dot{\boldsymbol{z}}$ to $\ddot{\boldsymbol{z}}$, and $f_k(\dot{\boldsymbol{z}})$ to $f_k(\ddot{\boldsymbol{z}})$. In particular, the quadrature integration (11) is now preformed over $\ddot{\boldsymbol{z}}$, and the total number of the nodes is reduced to $M = \prod_{j=2}^{N'} M_j$. This dimensionality reduction is critical for the pricing of Asian options as discussed later in § 5.

3.4. Forward price as control variate

When the quadrature nodes are too sparse, the error from the integration can be non-negligible. We can reduce this error using the forward price F_k as a control variate. Let $\bar{f}_k$ be the numerically evaluated expectation of $f_k(\dot{\boldsymbol{z}})$, $\bar{f}_k = \sum_{m=1}^{M} h_m f_k(\dot{\boldsymbol{z}}_m)$, which is not exactly equal to 1. For example, $E(e^{-\frac{1}{2}+z})$ for a standard normal z deviates by -6.3×10^{-3}, under the GHQ evaluation with three nodes, and by -4.6×10^{-4}, with four nodes, from the true value 1. As a result, F_k is mispriced by $F_k(\bar{f}_k - 1)$ under GHQ evaluation. This error is also present in the put-call parity of (11) and (12):

$$C - P - \sum_k (w_k F_k) + K = \sum_k w_k F_k(\bar{f}_k - 1), \tag{16}$$

which causes problems such as inconsistent implied volatilities for the put and call options with the same strike price. Since the sensitivity (delta) of each F_k is computed as (14), with little extra cost, we adjust the option prices by using them as the coefficients of the control variate:

$$C' = C - \sum_k D_k F_k(\bar{f}_k - 1), \quad P' = P - \sum_k (D_k - 1)F_k(\bar{f}_k - 1). \tag{17}$$

The put-call parity of the adjusted prices, C' and P', holds exactly.

4. Optimal choice of risk factor matrix

4.1. Illustrative example

Through a simple example, we demonstrate why a naive numerical integration suffers from slow convergence and how a proper rotation of the factor matrix can improve convergence. Let us consider a basket put option on two uncorrelated assets ($N = 2$) with parameters $\boldsymbol{\Sigma} = \boldsymbol{I}, r = 0, w_k = 1, F_k = e^{1/2}$, and $q_k = 0$ for $k = 1, 2$, so that the payoff is given as $(K - e^{x_1} - e^{x_2})^+$ for the independent standard normal RVs, x_1 and x_2. (We choose put option to more clearly illustrate the singularity from the vanishing exercise region. However, the same result holds for call option as well due to the put-call parity.) The put option price is:

$$P = \int P_{\text{BS}}(x_2)dx_2 \quad \text{for} \quad P_{\text{BS}}(x_2) = (K - e^{x_2})N(-d(x_2)) - e^{\frac{1}{2}}N(-d(x_2) - 1), \tag{18}$$

where $P_{\text{BS}}(x_2)$ is the integration of the payoff along the x_1 axis from $x_1 = -\infty$ to $-d(x_2) = \log(K - e^{x_2})$. As shown in Fig 1(a), the exercise boundary $-d(x_2)$ diverges to $-\infty$ as x_2 approaches $\log(K)$ from the left; thus, $P_{\text{BS}}(x_2) = 0$ for $x_2 \geq \log(K)$. In order to accurately evaluate the numerical integration over the x_2 axis, discretization should be dense around the singularity at $x_2 = \log(K)$.

Alternatively, let us consider the 45°-rotated coordinate (z_1, z_2), under which the payoff becomes $(K - e^{(z_1 - z_2)/\sqrt{2}} - e^{(z_1 + z_2)/\sqrt{2}})^+$. Then, we have the exercise boundary, $z_1 = -d(z_2) = -\sqrt{2}\log\left(2\cosh(z_2/\sqrt{2})/K\right)$ and the option price is:

$$P = \int P_{\text{BS}}(z_2)dz_2 \quad \text{for} \quad P_{\text{BS}}(z_2) = K\,N(-d(z_2)) - 2e^{\frac{1}{4}}\cosh(\frac{z_2}{\sqrt{2}})N(-d(z_2) - \frac{1}{\sqrt{2}}). \tag{19}$$

Since the boundary $-d(z_2)$ exists at all z_2, $P_{\text{BS}}(z_2)$ is infinitely differentiable in all z_2, suitable for the numerical integration along z_2 (see Fig 1(b) for $P_{\text{BS}}(x_2)$ and $P_{\text{BS}}(z_2)$.) As shown in Fig 1(c), the error from the quadrature integration under (z_2, z_1) exponentially decreases as we increase the number of nodes while the error under (x_2, x_1) decreases very slowly.

4.2. Selection of first factor

We generalize the above intuition to the correlated and higher dimensional cases. We set the following two criteria for the selection of $\boldsymbol{V}$: (i) the exercise boundary $d(\dot{\boldsymbol{z}})$ of (8) should exist for all $\dot{\boldsymbol{z}}$ and K, and (ii) the variation of $d(\dot{\boldsymbol{z}})$, $|\partial d(\dot{\boldsymbol{z}})/\partial z_j|$ for $j \geq 2$, should be minimized. Obviously, the purpose is to make $C_{\text{BS}}(\dot{\boldsymbol{z}})$ not only differentiable over $\dot{\boldsymbol{z}}$ without $-d(\dot{\boldsymbol{z}})$ diverging, but also as low varying as possible.

As the coefficient functions $\{f_k(\dot{\boldsymbol{z}})\}$ can take almost any arbitrary positive values, we impose $w_k V_{k1} > 0$ for all k as a sufficient condition to satisfy (i). With this constraint, the left-hand side of (8) is a strictly monotonic function of z_1, with the value range being $(0, \infty)$ for basket and Asian

Figure 1 The pricing of the basket put option with payoff $(K - e^{x_1} - e^{x_2})^+$ for uncorrelated standard normals, x_1 and x_2. In (a) we show the exercise region for $K = 2$ and 4 (shaded area) along with the boundary $-d(x_2)$ (solid line). The axes (z_2, z_1) is 45° degree rotation from the original axes (x_2, x_1). In (b) we show the integration along the first dimension of the two coordinate systems, x_1 (solid blue) and z_1 (dashed red). In (c) we show the error of the GHQ integration of the functions in (b) under (x_2, x_1) (diamond) and under (z_2, z_1) (circle), for increasing node size.
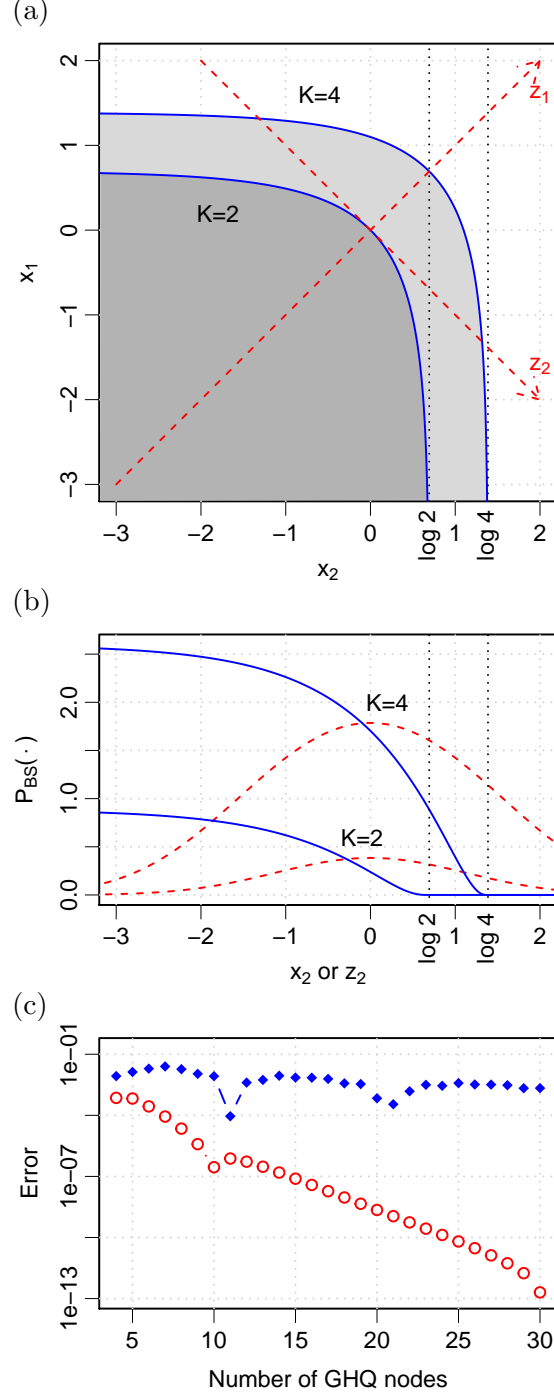
options, or $(-\infty, \infty)$ for spread options. Hence, a unique root $d(\dot{\boldsymbol{z}})$ exists for any $\dot{\boldsymbol{z}}$ and non-trivial K.

For (ii), we apply the linearized approximation of the GBM, $\exp(-\frac{1}{2}V_{kj}^2 + V_{kj}z_j) \approx 1 + V_{kj}z_j$, assuming a small variance, $\|\boldsymbol{V}\|_F \ll 1$. After ignoring the terms of the second order and higher, (8) approximates to:

$$\sum_k w_k F_k + \sum_k w_k F_k (\boldsymbol{V}_{k*}\dot{\boldsymbol{z}} + V_{k1}z_1) = K, \tag{20}$$

and we obtain $\partial d(\dot{\boldsymbol{z}})/\partial z_j$ as the following constant:

$$\frac{\partial\, d(\dot{\boldsymbol{z}})}{\partial\, z_j} \approx \frac{\boldsymbol{g}^T \boldsymbol{V}_{*j}}{\boldsymbol{g}^T \boldsymbol{V}_{*1}} = \frac{\boldsymbol{g}^T \boldsymbol{C}\, \boldsymbol{Q}_{*j}}{\boldsymbol{g}^T \boldsymbol{C}\, \boldsymbol{Q}_{*1}} \quad \text{for} \quad j \geq 2. \tag{21}$$

Here, $\boldsymbol{g}$ is the normalized forward-adjusted weight vector, $g_k \propto w_k F_k$ with $|\boldsymbol{g}| = 1$. The partial derivatives are minimized to zero when $\boldsymbol{Q}_{*1}$ is aligned to the direction of $\boldsymbol{C}^T \boldsymbol{g}$ because the choice maximizes the denominator and makes the numerator zero, due to the orthogonality between $\boldsymbol{Q}_{*1}$ and $\boldsymbol{Q}_{*j}$ for $j \geq 2$. Therefore, we have the optimal first factor:

$$\boldsymbol{Q}_{*1} = \frac{\boldsymbol{C}^T \boldsymbol{g}}{\sqrt{\boldsymbol{g}^T \boldsymbol{\Sigma} \boldsymbol{g}}} \quad \text{and} \quad \boldsymbol{V}_{*1} = \boldsymbol{C}\, \boldsymbol{Q}_{*1} = \frac{\boldsymbol{\Sigma} \boldsymbol{g}}{\sqrt{\boldsymbol{g}^T \boldsymbol{\Sigma} \boldsymbol{g}}}. \tag{22}$$

This is equivalent to rotating the z_1 axis to the steepest ascending direction of the left-hand side of (20), which is in agreement with the observation from § 4.1. The other axes span slowly varying dimensions, which are subject to costly numerical integrations. This way, the overall computation cost is minimized.

However, $\boldsymbol{V}_{*1}$ in (22) does not always conform to the earlier constraint $w_k F_k > 0$. In the case of $w_k V_{k1} \leq 0$ for some k, we adjust V_{k1} by pushing it into the conforming region by:

$$V_{k1}^{(\mathrm{adj})} = \begin{cases} \mu V_{k1} & \text{if} \quad w_k V_{k1} > 0 \\ \mu\, \varepsilon\, \mathrm{sign}(w_k)\sqrt{\Sigma_{kk}} & \text{if} \quad w_k V_{k1} \leq 0, \end{cases} \tag{23}$$

for a small $\varepsilon > 0$ and rescaling factor $\mu > 0$, making $\boldsymbol{Q}_{*1} = \boldsymbol{C}^{-1}\boldsymbol{V}_{*1}^{(\mathrm{adj})}$ a unit vector ($\mu = 1$ if no adjustment). We use $\sqrt{\Sigma_{kk}}$ as a characteristic scale of V_{k1} because $|V_{k1}| \leq \sqrt{\Sigma_{kk}}$.

4.3. Remaining factors

We determine the remaining columns, $\boldsymbol{V}_{*j}$ for $j \geq 2$, using singular value decomposition (SVD), by which the columns are rearranged orthogonal and in decreasing order of factor strength $|\boldsymbol{V}_{*j}|$. This process can be completed in the two steps. We, first, find any orthonormal rotation matrices, whose first columns are the same as the selected $\boldsymbol{Q}_{*1}$. The computationally lightest choice is the Householder reflection matrix $\boldsymbol{R}$, which maps $\boldsymbol{e}_1 = (1, 0, \cdots)^T$ to $\boldsymbol{Q}_{*1}$ using a mirror image:

$$\boldsymbol{R} = \boldsymbol{I} - 2\boldsymbol{v}\boldsymbol{v}^T \quad \text{where} \quad \boldsymbol{v} = (\boldsymbol{Q}_{*1} - \boldsymbol{e}_1)/|\boldsymbol{Q}_{*1} - \boldsymbol{e}_1|. \tag{24}$$

As a result, the first column of $\boldsymbol{CR}$ is the same as $\boldsymbol{V}_{*1}$. Next, we rearrange the remaining columns of $\boldsymbol{CR}$ via the reduced-size SVD, $\boldsymbol{C}\left(\boldsymbol{R}_{*2} \;\cdots\; \boldsymbol{R}_{*N}\right) = \dot{\boldsymbol{U}}\,\dot{\boldsymbol{D}}\,\dot{\boldsymbol{Q}}^T$, where $\dot{\boldsymbol{D}}$ is an $(N-1)\times(N-1)$ diagonal matrix with the (non-negative) singular values in decreasing order, and $\dot{\boldsymbol{U}}$ and $\dot{\boldsymbol{Q}}$ are the $N\times(N-1)$ and $(N-1)\times(N-1)$ matrices, respectively, satisfying $\dot{\boldsymbol{U}}^T\dot{\boldsymbol{U}} = \dot{\boldsymbol{Q}}^T\dot{\boldsymbol{Q}} = \boldsymbol{I}$. We, finally, obtain the full $\boldsymbol{V}$ by column-wise concatenation:

$$\boldsymbol{V} = (\boldsymbol{V}_{*1}\;\dot{\boldsymbol{U}}\dot{\boldsymbol{D}}), \tag{25}$$

and the corresponding $\boldsymbol{Q}$ as:

$$\boldsymbol{Q} = \boldsymbol{R}\begin{pmatrix} 1 & \boldsymbol{0}^T \\ \boldsymbol{0} & \dot{\boldsymbol{Q}} \end{pmatrix}, \tag{26}$$

where $\boldsymbol{0}$ is the zero vector. Due to the linearized assumption, our choice of $\boldsymbol{V}$ is independent from the strike price K, so that if $\boldsymbol{V}$ is computed once, it can be used for options with multiple strike prices.

5. Remarks on Asian options

In this section, we discuss a few implications of our method in the context of Asian options. First, because the covariance $\boldsymbol{\Sigma}$ is from the self-correlation within a Brownian motion, the Cholesky decomposition $\boldsymbol{C}$ is trivially computed as:

$$C_{kj} = \begin{cases} 0 & \text{if} \quad k < j \\ \sigma\sqrt{t_j - t_{j-1}} & \text{if} \quad k \geq j \quad (t_0 = 0). \end{cases}$$

Therefore, it does not bear a computational burden for large N.

Second, all elements of $\boldsymbol{V}_{*1}$ in (22) are positive because all elements of $\boldsymbol{\Sigma}$ and $\boldsymbol{g}$ are positive for Asian options. As such, the selected $\boldsymbol{V}_{*1}$ is not compromised by the adjustment step of (23).

Third, the columns of the factor matrix $\boldsymbol{V}$ can be interpreted as a series representation of a Brownian motion $\sigma W(t)$ on a discretized time set $\{t_k\}$, $\sigma\left(W(t_1), \cdots, W(t_N)\right)^T \overset{d}{=} \boldsymbol{V}\boldsymbol{z}$. If $V_j(t)$ is the continuum limit of V_{kj}, as $N \to \infty$ with $t = k/N$ fixed, for $\sigma = 1$, the set $\{V_j(t)\}$ serves as a series expansion of $W(t)$:

$$W(t) \overset{d}{=} \sum_{j=1}^{\infty} V_j(t)\, z_j, \tag{27}$$

for independent standard normals $\{z_j\}$. Therefore, it is worth comparing this expansion to the well-known Karhunen–Loève expansions:

$$W(t) \overset{d}{=} \sum_{j=1}^{\infty} V_j^{(\text{KL})}(t)\, z_j \quad \text{for} \quad V_j^{(\text{KL})}(t) = \frac{\sqrt{2}}{(j-\frac{1}{2})\,\pi} \sin\left((j-\frac{1}{2})\pi t\right). \tag{28}$$

Figure 2 shows the first three factors from the two expansions. While the terms are similar, we note a subtle difference in the first factor. For the normalized parameters, that is, $\sigma = 1$, $t_k = k/N$ ($T = 1$), $w_k = 1/N$, and $r = q = 0$, $V_1(t)$ is given by the continuous version of (22):

$$V_1(t) = \frac{\int_0^1 \min(t, u) du}{\sqrt{\int_0^1 \int_0^1 \min(s, u) du ds}} = \sqrt{3}\left(t - \frac{1}{2}t^2\right). \tag{29}$$

Since the Karhunen–Loève expansion is the PCA of $W(t)$ in functional space, $V_1^{(\mathrm{KL})}(t)$ is chosen to maximize the L^2-norm, $\int_0^1 V_1^2(t) dt$. Therefore, $\|V_1^{(\mathrm{KL})}(t)\|_2 = 2/\pi \,(\approx 0.6366)$ is larger than $\|V_1(t)\|_2 = \sqrt{2/5}\,(\approx 0.6325)$. On the other hand, our method of choosing $V_1(t)$ is to maximize $\int_0^1 V_1(t) dt$. Thus, $\int_0^1 V_1(t)\, dt = 1/\sqrt{3}\,(\approx 0.5774)$ is larger than $\int_0^1 V_1^{(\mathrm{KL})}(t)\, dt = 4\sqrt{2}/\pi^2\,(\approx 0.5732)$. The continuous representation (29) is only valid under constant weight, and it no longer holds if, for example, $r \neq 0$ or w_k is not constant. Therefore, in general, we numerically compute $\boldsymbol{V}_{*1}$ rather than using (29).

Fourth, the dimensionality reduction is critically effective in Asian options since the dimension N is large. For one-year maturity, the monthly averaging corresponds to $N = 12$, weekly averaging to $N = 50$, and daily averaging to $N = 250$, approximately. Even if we use a few nodes per dimension, the total number of nodes becomes prohibitively large. However, the first several factors explain most of variance, and the remaining factors have little impact on the option price. Table 1 shows the portion of the explained variance, $\sum_{j=1}^{N'} |\boldsymbol{V}_{*j}|^2 / \|\boldsymbol{V}\|_F^2$, as a function of increasing N'. The first factor, $\boldsymbol{V}_{*1}$, accounts for the largest part, about 80%, and the cumulative portion reaches about 96% at $N' = 5$. In the numerical results in § 6, we will indeed show that the five dimensions, one under analytic and four under numerical integration, are sufficient for accurate option pricing. If the purpose of the averaging feature is to avoid market manipulation, as is often the case, the averaging starts in a forward time near maturity. Because the overall correlation in this case is higher than in that of immediate averaging, the explained variance portion is higher and the dimensionality reduction is more effective.

Lastly, the valuation of continuously monitored Asian options is cast into discrete monitoring. For a better convergence of the integration over time, we use the weights by Simpson's rule rather than constant weights. For a discretization step ΔT, such that $N = T/\Delta T$ is even, the observation time and weights are given as:

$$t_k = k\Delta T, \quad w_k = \begin{cases} 4\Delta T/(3T) & \text{if } k \text{ is odd} \\ 2\Delta T/(3T) & \text{if } k \text{ is even} \end{cases} \quad \text{for} \quad 0 \leq k \leq N, \tag{30}$$

with the exception of the weights at the two end points, $w_0 = w_N = \Delta T/(3T)$.

Figure 2 First three terms of series expansions of standard Brownian motion. The solid (blue) lines are the factors $V_j(t)$ from our method computed with $N = 50$, while the dashed (red) lines are the factors $V_j^{(\mathrm{KL})}(t)$ from the Karhunen-Loève expansions in (28).
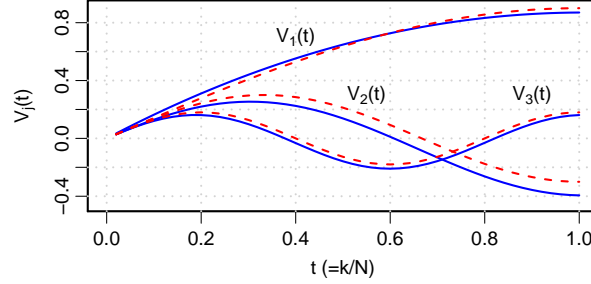
Table 1 Ratio of explained variance in percent (%) as function of first N' dimensions. We assume $r = q = 0$ and $w_k = 1/N$.

$N \setminus N'$	1	2	3	4	5
12	80	90	94	96	97
50	80	90	93	95	96
250	80	90	93	95	96

Table 2 Parameter sets for test cases. The parameter noted by $*$ is to be varied in the test, and the value superscripted by $*$ is the base value when not varied.

Label	N	t_k or T	$S_k(0)$	K	w_k	$\sigma_k\,(\%)$	$\rho_{k \neq j}\,(\%)$	$q_k\,(\%)$	$r\,(\%)$
	References that test same parameter set								
S1	2	1	$(100, 96)$	$*$	$(1, -1)$	$(20, 10)$	50	5	10
	Dempster and Hong (2002), Hurd and Zhou (2010), Caldana and Fusai (2013)								
S2	2	1	$(200, 100)$	100	$(1, -1)$	$(15, 30)$	$*$	0	0
	No previous reference								
B1	4	5	100	100^*	$1/4$	40^*	50^*	0	0
	Krekel et al. (2004), Caldana et al. (2016)								
B2	7	$*$	100	$*$	Table 3				6.3
	Milevsky and Posner (1998b), Zhou and Wang (2008)								
A1	50	$k/50\,(k \geq 0)$	100	$*$	$1/51$	$*$	$\cdot$	0	10
	Levy and Turnbull (1992), Benhamou (2002), Černỳ and Kyriakou (2011)								
A2	$*$	$k/N\,(k \geq 0)$	100	$*$	$1/(N+1)$	17.801	$\cdot$	0	3.67
	Fusai and Meucci (2008), Černỳ and Kyriakou (2011), Fusai et al. (2011), Cai et al. (2013), Zhang and Oosterlee (2013)								

Table 3 Remaining parameters for B2

w_k	$\sigma_k(\%)$	$\rho_{kj}(\%)$ for $k < j$						$q_k(\%)$
0.10	11.55	35	10	27	4	17	71	1.69
0.15	20.68		39	27	50	-8	15	2.39
0.15	14.53			53	70	-23	9	1.36
0.05	17.99				46	-22	32	1.92
0.20	15.59					-29	13	0.81
0.10	14.62						-3	3.62
0.25	15.68							1.66

6. Numerical results

Our method is implemented in R (Ver. 3.3.2, 64-bit) on a personal computer running the Windows 10 operating system with an Intel core i5 2.2 GHz CPU and 8 GB RAM. We test seven parameter sets, the first six of which are described in Tables 2 and 3. The sets are labeled with **S** for spread, **B** for basket, and **A** for Asian options. The set **A3** for the continuously monitored Asian option is separately displayed in Table 12, along with the results. Except for the set **S2**, we select the parameters repeatedly used in previous studies for easier comparison.

The numerical results are reported in Tables 4∼12. Except for the three Asian option sets, we compute two versions of the prices. One version is the "fast" price, for which we use minimal GHQ nodes targeted with the practically sufficient precision of 3∼4 decimals. The computational cost for the fast price is inexpensive. The other version is the converged price, against which we measure the error of the fast price. The converged price is obtained within our method as the node sizes are increased. We target seven-decimal precision for the converged price. For the Asian option cases (Tables 10∼12), we only report the fast price, and the error is measured from the previous studies, Černỳ and Kyriakou (2011) for the discrete cases (**A1** and **A2**) and Linetsky (2004) for the continuous case (**A3**). All prices in the tables are the present values of the call options, that is, the forward value discounted by e^{-rT}.

In some tables, we also show the used factor matrix $\boldsymbol{V}$ in the following representation to provide extra properties in addition to the matrix itself.

$$
\begin{array}{c|ccc|c}
\boldsymbol{g}^T\boldsymbol{V}_{*1} & |\boldsymbol{V}_{*1}| & \cdots & |\boldsymbol{V}_{*N}| & \|\boldsymbol{V}\|_F = (\sum_k \Sigma_{kk})^{1/2} \\
\hline
g_1 & V_{11} & \cdots & V_{1N} & |\boldsymbol{V}_{1*}| = \sqrt{\Sigma_{11}} \\
\vdots & \vdots & V_{kj} & \vdots & \vdots \\
g_N & V_{N1} & \cdots & V_{NN} & |\boldsymbol{V}_{N*}| = \sqrt{\Sigma_{NN}} \\
\hline
& \cdot & M_2 \cdots & M_N & M = \prod_{j \geq 2} M_j
\end{array}
\tag{31}
$$

The center is $\boldsymbol{V}$ itself. The upper and right panel shows the L^2-norm of the columns and rows, respectively, and the upper right corner is the Frobenius norm. In the left panel is the forward-adjusted weight vector $\boldsymbol{g}$ and, in the upper left corner, the dot product $\boldsymbol{g}^T\boldsymbol{V}_{*1}$. The lower panel shows the node size M_j for the j-th dimension for $j \geq 2$, with the total size M in the lower right corner.

In implementation, it is important to choose M_j in an economic manner. The node sizes do not have to be same for all dimensions. We, rather, want to select M_j, so that all dimensions evenly achieve a similar level of accuracy. A general guideline is that the density of the nodes should be proportional to $|\partial d(\dot{\boldsymbol{z}})/\partial z_j|$, in order to properly capture the change in $d(\dot{\boldsymbol{z}})$. To this extent, we use the following rule to systematically determine M_j in our tests:

$$
M_j = \left[\frac{|\boldsymbol{V}_{*j}|}{|\boldsymbol{g}^T\boldsymbol{V}_{*1}|} \lambda + 1 \right] \quad \text{for} \quad j \geq 2,
\tag{32}
$$

where $[x]$ is the nearest integer of x and λ is the coefficient for the level of accuracy. The ratio $|\boldsymbol{V}_{*j}|/|\boldsymbol{g}^T\boldsymbol{V}_{*1}|$ is obtained by applying the Cauchy-Schwarz inequality, $|\boldsymbol{g}^T\boldsymbol{V}_{*j}| < |\boldsymbol{g}| \cdot |\boldsymbol{V}_{*j}| = |\boldsymbol{V}_{*j}|$, to (21), thus understood as an approximate upper bound of $|\partial d(\dot{\boldsymbol{z}})/\partial z_j|$. This rule also serves as the criteria for the dimension reduction: if $M_j = 1$ for some j, we truncate the dimension according to § 3.3. Moreover, this rule is independent from K, so that if $\{\dot{\boldsymbol{z}}_m\}$ and $\{w_m\}$ are computed once, they can be used for options with multiple values of K. For Asian options, however, we empirically find that $M_j = 3$ for $2 \leq j \leq 5$ ($M = 81$) works very well; thus, we do not resort to (32).

6.1. Spread options

In **S1**, we price the spread call options for varying strikes from $K = 0$ (in-the-money) to 4 (at-the-money). To see the speed of convergence, we increase the node size for the second dimension from $M_2 = 2$. As shown in Table 4, the convergence is extremely fast. While the prices with $M_2 = 2$ are already accurate, they converge within seven decimals at $M_2 = 3$. The table also shows that the control variate correction of § 3.4 further reduces error. While Hurd and Zhou (2010) and Caldana and Fusai (2013) show accuracy similar to the $M_2 = 3$ result, their methods have to evaluate the expensive Fourier inversion in two and one dimensions, respectively. The risk factor matrix is presented in Table 4(b). In this example, the adjustment step (23) is triggered for V_{21} with $\varepsilon = 0.01$. In addition, we independently implement the analytic approximation methods of Bjerksund and Stensland (2014), Lo (2015), and Li et al. (2008) for the spread options. (For Lo (2015), the "Strang's splitting approximation I" method in the reference is implemented, which is given in an explicit formula.) All three methods work well on **S1**, showing the error in the order of 10^{-6} or less.

In **S2**, we price at-the-money spread call options for varying correlation ρ_{12} from 90% to -90%. The results are shown in Table 5(a). This parameter set is designed for the first asset to follow a displaced GBM, $dS_1(t) = \sigma_1(S_1(t) + L) \, dW_1(t)$ with $L = 100$, to exhibit a negative implied volatility skew. Therefore, the true parameters are similar to those of S_2, as $S_1(0) = 100$ and $\sigma_1 \approx 30\%$, and $K = 100$ corresponds to the at-the-money strike. As ρ_{12} changes, so does $\boldsymbol{V}$. We use (32) to determine M_2. For the fast price, we use $\lambda = 3$, so that M_2 varies from 17 to 2. Since the components in $\boldsymbol{V}_{*1}$ must have opposite signs for spread options, its norm weakens under positive correlation, thus requiring denser nodes. The quadrature size rule (32) works reasonably well, although it tends to over-allocate nodes under high correlation. The price quickly converges as λ is increased, and the seven-decimal precision is reached at $\lambda = 9$. We show $\boldsymbol{V}$ for $\rho_{12} = 90\%$ and -90% in Table 5(b) and (c), respectively. It is worth noting that the two columns switch places with a sign change. The performance of the analytic approximation methods is worse in **S2**, probably because of the displaced GBM feature, that is, the significant difference in the spot prices and big strike price.

Table 4 Numerical results for **S1**: (a) the converged prices (CPs) and fast price errors (FP Err) with and without a control variate for varying K, and (b) the factor matrix V (see (31) for the representation).

(a)

K	CP	FP Err w/ CV		FP Err w/o CV	
	$M_2 = 4$	$M_2 = 3$	$M_2 = 2$	$M_2 = 3$	$M_2 = 2$
0.0	8.5132252	-7.4e-9	-3.0e-6	-1.3e-7	-1.1e-4
0.4	8.3124607	-8.2e-9	-3.5e-6	-1.3e-7	-1.1e-4
0.8	8.1149938	-9.0e-9	-4.0e-6	-1.3e-7	-1.1e-4
1.2	7.9208198	-9.8e-9	-4.7e-6	-1.3e-7	-1.1e-4
1.6	7.7299325	-1.1e-8	-5.3e-6	-1.3e-7	-1.1e-4
2.0	7.5423239	-1.1e-8	-6.0e-6	-1.3e-7	-1.1e-4
2.4	7.3579843	-1.2e-8	-6.7e-6	-1.3e-7	-1.1e-4
2.8	7.1769024	-1.2e-8	-7.5e-6	-1.3e-7	-1.1e-4
3.2	6.9990651	-1.3e-8	-8.2e-6	-1.3e-7	-1.1e-4
3.6	6.8244581	-1.3e-8	-9.0e-6	-1.3e-7	-1.1e-4
4.0	6.6530651	-1.3e-8	-9.7e-6	-1.3e-7	-1.1e-4

(b)

0.125	0.172	0.143	0.224
0.721	0.172	0.102	0.200
-0.693	-0.001	0.100	0.100
	$\cdot$	4	4

Table 5 Numerical results for **S2** with varying correlation ρ_{12}. The converged prices (CPs) and fast price errors (FP Err) are shown in (a). The fast prices are obtained with $\lambda = 3$ and converged price with $\lambda = 9$. The errors of three approximation methods are also displayed for reference: Bjerksund and Stensland (2014) (BjSt Err), Lo (2015) (Lo Err), and Li et al. (2008) (LDZ Err). The factor matrices V for $\rho_{12} = 90\%$ and -90% are displayed in (b) and (c), respectively.

(a)

ρ_{12} (%)	CP	FP Err	M_2	BjSt Err	Lo Err	LDZ Err
90	5.4792720	-1.5e-8	17	-1.3e-1	$+1.4$e-2	-1.9e-2
70	9.3209439	$+3.7$e-8	10	-6.3e-2	$+1.0$e-2	-1.0e-4
50	11.9804918	$+2.2$e-7	7	-4.0e-2	$+1.0$e-2	$+7.9$e-4
30	14.1425869	-4.0e-7	6	-2.8e-2	$+8.8$e-3	$+7.7$e-4
10	16.0102190	-1.4e-7	5	-2.0e-2	$+6.6$e-3	$+6.1$e-4
-10	17.6770249	$+5.2$e-6	4	-1.6e-2	$+3.7$e-3	$+4.5$e-4
-30	19.1954201	$+1.5$e-6	4	-1.4e-2	-3.6e-5	$+3.1$e-4
-50	20.5982705	-8.0e-6	3	-1.3e-2	-4.3e-3	$+1.9$e-4
-70	21.9077989	-1.7e-6	3	-1.4e-2	-9.2e-3	$+1.0$e-4
-90	23.1398674	-8.3e-5	2	-1.5e-2	-1.5e-2	$+2.0$e-5

(b)

0.060	0.075	0.327	0.335
0.894	0.034	0.146	0.150
-0.447	-0.067	0.292	0.300
	$\cdot$	17	17

(c)

0.262	0.327	0.075	0.335
0.894	0.146	0.034	0.150
-0.447	-0.292	0.067	0.300
	$\cdot$	2	2

Although the method of Li et al. (2008) is notably more accurate than the other two methods, it illustrates the limitation of analytic approximation.

Table 6 Numerical results for **B1** with varying K: (a) the converged prices (CPs) and fast price errors (FP Err), and (b) the factor matrix V. The fast prices are obtained using $\lambda = 9$, which results in $M_{j \geq 2} = 5$ ($M = 125$).

(a)

K	CP	FP Err
50	54.3101761	-2.0e-4
60	47.4811265	-2.5e-4
70	41.5225192	-2.6e-4
80	36.3517843	-2.4e-4
90	31.8768032	-2.0e-4
100	28.0073695	-1.3e-4
110	24.6605295	-6.4e-5
120	21.7625789	$+8.4$e-6
130	19.2493294	$+7.9$e-5
140	17.0655420	$+1.4$e-4
150	15.1640103	$+2.0$e-4

(b)

1.414	1.414	0.632	0.632	0.632	0.000
0.500	0.707	-0.000	-0.420	0.352	0.894
0.500	0.707	-0.000	-0.191	-0.513	0.894
0.500	0.707	-0.447	0.306	0.081	0.894
0.500	0.707	0.447	0.306	0.081	0.894
	$\cdot$	5	5	5	125

6.2. Basket Option

The parameter sets **B1** and **B2** are frequently used benchmarks in previous studies. Here we report the convergent option values for the first time. The parameter set **B1** is extracted from Krekel et al. (2004), where the performances of several analytic approximation methods are compared. In Tables 6 and 7, we show the results for varying K and $\rho_{k \neq j}$, respectively, from the base parameter values. Moreover, in Table 8, we test the inhomogeneous volatilities by varying σ_k simultaneously for $1 \leq k \leq 3$ with $\sigma_4 = 100\%$ fixed. In all tests, we obtain consistent fast prices with $\lambda = 9$. Our fast prices are more accurate than the benchmark Monte Carlo prices of Krekel et al. (2004), and the computation cost is much cheaper. In the test of Table 6, $\lambda = 9$ corresponds to $M_j = 5$ per dimension ($M = 125$). In addition, the node sizes in Tables 7 and 8 are shown in their respective last columns. Contrary to a spread option, lower correlation requires denser nodes in a basket option. (In the test, the lower bound of the correlation $\rho_{k \neq j}$ is -33.33% for the covariance matrix to be positive-semidefinite.) It is remarkable that only a few nodes per dimension produce accurate prices in the inhomogeneous volatility test. No approximation method shows satisfactory precision in the same test (Krekel et al. 2004).

The parameter set **B2** is the so-called G-7 indices basket option tested in Milevsky and Posner (1998b) and Zhou and Wang (2008). The call option prices for varying K and T in Table 9(a) and the factor matrix V are shown in Table 9(b). Our method works well for this $N = 7$ case. The error of the fast prices ($\lambda = 3$, $M = 432$) are in the order of 10^{-4} at most, which is smaller than the standard error of the Monte Carlo simulation in Zhou and Wang (2008). The seven-digit convergent prices are computed with $\lambda = 12$ and $M \approx 1.2 \times 10^5$.

Table 7   Numerical results for **B1** parameter set with varying correlation $\rho_{k \neq j}$ simultaneously. The converged prices (CPs), fast price error (FP Err), and quadrature sizes are shown. The fast prices are obtained using $\lambda = 9$.

$\rho_{k \neq j} (\%)$	CP	FP Err	$M_{j \geq 2}(M)$
-10	17.7569163	-4.9e-8	12, 12, 12 (1728)
10	21.6920965	-7.3e-6	7, 7, 7 (343)
30	25.0292992	$+1.3$e-4	6, 6, 6 (216)
50	28.0073695	-1.2e-4	5, 5, 5 (125)
80	32.0412265	-4.0e-4	3, 3, 3 (27)
95	33.9186874	-3.1e-3	2, 2, 2 (8)

Table 8   Numerical results for **B1** with varying volatilities $\sigma_{k \leq 3}$, with $\sigma_4 = 100\%$ fixed: (a) the converged prices (CPs), fast price errors (FP Err), and node sizes, and (b) the factor matrix $\boldsymbol{V}$ for the case of $\sigma_{k \leq 3} = 10\%$. The fast prices are obtained using $\lambda = 9$.

(a)

$\sigma_{k \leq 3}(\%)$	CP	FP Err	$M_{j \geq 2}(M)$
5	19.4590950	-4.3e-4	3, 2, 2 (12)
10	20.9682321	$+8.4$e-4	4, 2, 2 (16)
20	25.3794239	$+6.9$e-4	5, 3, 3 (45)
40	36.0485407	$+1.6$e-3	6, 4, 4 (96)
60	46.8189186	$+6.5$e-3	6, 4, 4 (96)
80	56.7772198	-9.2e-3	5, 5, 5 (125)
100	65.4256003	$+1.8$e-4	5, 5, 5 (125)

(b)

1.304	2.217	0.429	0.158	0.158	2.269
0.500	0.134	-0.124	0.129	-0.011	0.224
0.500	0.134	-0.124	-0.054	0.117	0.224
0.500	0.134	-0.124	-0.074	-0.106	0.224
0.500	2.205	0.371	-0.000	-0.000	2.236
	$\cdot$	4	2	2	16

6.3. Asian options

We test three parameter sets for Asian options. The results for the discrete monitoring sets, **A1** and **A2**, are reported in Tables 10 and 11, respectively. (A parameter set, which is almost the same as **A1** except for $r = 4\%$, has been popularly tested in the literature such as Černỳ and Kyriakou (2011), Fusai et al. (2011) and Cai et al. (2013). Since the option prices from the two sets are notably different, they should not be confused.) In Table 10, we vary K and σ, whereas in Table 11, we vary K and N. The errors are measured from Černỳ and Kyriakou (2011), where the results are reported with the accuracy of 10^{-7}. The fast prices computed with only 81 nodes over four dimensions ($M_j = 3$ for $2 \leq j \leq 5$) have errors in the order of 10^{-4} or less. The overall underpricing is due to the decrease in variance from the dimensionality reduction. In **A1** and **A2**, the average computation time per one option price is 0.01, 0.02, and 0.06 seconds for $N = 12$, 50, and 250, respectively. It can be further accelerated when the prices for multiple values of K are computed together because the computations for $\boldsymbol{V}$, $\{\dot{\boldsymbol{z}}_m\}$, and $\{h_m\}$ are not to be repeated. Although a

Table 9   Numerical results for **B2** with varying K and T: (a) the converged prices (CPs) and fast price errors (FP Err), and (b) the factor matrix $\boldsymbol{V}$ for the $T = 1$ case.

(a)

K	CP ($\lambda = 12$)				FP Err ($\lambda = 3$)			
	$M_{j \geq 2} = (11, 10, 8, 7, 5, 4)$, $M = 123200$				$M_{j \geq 2} = (4, 3, 3, 3, 2, 2)$, $M = 432$			
	$T = 0.5$	$T = 1$	$T = 2$	$T = 3$	0.5	1	2	3
80	21.6022546	23.1411627	26.0424328	28.6992602	-1.6e-8	-9.0e-7	-1.0e-5	-2.8e-5
100	3.8828353	6.2216810	10.2156012	13.7425580	-4.3e-5	-1.1e-4	-2.5e-4	-3.7e-4
120	0.0235189	0.3535584	2.0570044	4.4578389	-5.8e-6	-7.9e-5	-4.1e-4	-7.8e-4

(b)

0.23	0.26	0.20	0.17	0.14	0.12	0.08	0.06	0.42
0.24	0.07	-0.06	-0.01	-0.03	0.02	-0.03	0.05	0.12
0.36	0.14	0.05	0.12	-0.05	0.05	0.00	-0.01	0.21
0.36	0.09	0.08	-0.02	0.04	-0.02	-0.06	-0.01	0.15
0.12	0.10	0.06	-0.10	0.00	0.09	0.01	0.00	0.18
0.49	0.11	0.09	0.00	0.02	-0.05	0.04	0.02	0.16
0.24	0.00	-0.09	0.05	0.10	0.03	0.01	0.00	0.15
0.61	0.10	-0.09	-0.06	-0.05	-0.02	0.01	-0.02	0.16
	$\cdot$	4	3	3	3	2	2	432

Table 10   Numerical results for **A1** with varying strike price K and volatility σ. The fast prices (FPs) with $M_{2 \leq j \leq 5} = 3$ and errors (Err) are shown. The errors are measured from Černỳ and Kyriakou (2011), where the values are reported using seven-decimal precision.

| K | FP | | | Err ($\times 10^{-7}$) | | |
	$\sigma = 10\%$	$\sigma = 30\%$	$\sigma = 50\%$	10%	30%	50%
80	22.7771749	23.0914273	24.8242382	0	-105	-199
90	13.7337771	15.2207525	18.3316585	-2	-85	-155
100	5.2489922	9.0271796	13.1580058	-5	-92	-398
110	0.7238317	4.8348903	9.2344356	-7	-168	-778
120	0.0264089	2.3682616	6.3718411	-3	-238	-1125

direct comparison on CPU time is difficult due to different computing environments, Černỳ and Kyriakou (2011) report 1 to 0.3 seconds, as σ varies from 10% to 50%, for computing $N = 50$ case with five-decimal precision. In Table 12, we report the result for the continuous monitoring set **A3**. We discretize time with $\Delta T = 1/200$; hence, $N = 200$ for $T = 1$ and $N = 400$ for $T = 2$. The fast prices computed with 81 nodes match well to the values of Linetsky (2004), computed with up to 10-decimal accuracy. The computation time per one option is 0.04 and 0.18 seconds for $N = 200$ and 400 cases, respectively.

7. Conclusion

The option pricing under a multivariate BSM model is a challenging problem with a long history of research, due to the curse of dimensionality. We substantially ease this curse by replicating the option price as a weighted sum of single-factor BSM prices, under an optimally rotated state space.

Table 11 Numerical results for **A2** for varying strike price K and the number of observations N. The fast prices (FPs) with $M_{2 \le j \le 5} = 3$ and errors (Err) are shown. The errors are measured from Černỳ and Kyriakou (2011), where the values are reported using seven-decimal precision.

K	FP			Err ($\times 10^{-7}$)		
	$N = 12$	$N = 50$	$N = 250$	12	50	250
90	11.9049132	11.9329355	11.9405604	-25	-27	-28
100	4.8819577	4.9372004	4.9521546	-39	-24	-23
110	1.3630326	1.4025110	1.4133626	-54	-45	-44

Table 12 Parameters and numerical results for **A3**. For all seven cases, $K = 2$ and $q = 0$. The continuous monitoring is discretized by Simpson's rule (30) with $\Delta T = 1/200$. The fast prices (FPs) are computed with $M_{2 \le j \le 5} = 3$ and the errors (Err) are measured from Linetsky (2004), where the values are reported using 10-decimal precision.

Case	T	S_0	$\sigma(\%)$	$r(\%)$	FP	Err ($\times 10^{-7}$)
1	1	2.0	10	2	0.0559862	2
2	1	2.0	30	18	0.2183878	3
3	2	2.0	25	1.25	0.1722685	-2
4	1	1.9	50	5	0.1931733	-5
5	1	2.0	50	5	0.2464156	-1
6	1	2.1	50	5	0.3062206	2
7	2	2.0	50	5	0.3500929	-24

Moreover, this method can be uniformly applied to spread, basket, and Asian options. Numerical examples show that this method is both fast and accurate.

References

Beisser, Jochen. 1999. Another way to value basket options. Tech. rep., Working paper, Johannes Gutenberg-Universität Mainz.

Benhamou, Eric. 2002. Fast Fourier transform for discrete Asian options. *Journal of Computational Finance* **6**(6) 49–68.

Bjerksund, Petter, Gunnar Stensland. 2014. Closed form spread option valuation. *Quantitative Finance* **14**(10) 1785–1794.

Borovkova, Svetlana, Ferry J Permana, Hans VD Weide. 2007. A closed form approach to the valuation and hedging of basket and spread option. *The Journal of Derivatives* **14**(4) 8–24.

Broadie, Mark, Jerome B Detemple. 2004. Anniversary article: option pricing: valuation models and applications. *Management science* **50**(9) 1145–1177.

Broadie, Mark, Özgür Kaya. 2006. Exact simulation of stochastic volatility and other affine jump diffusion processes. *Operations Research* **54**(2) 217–231.

Cai, Ning, Nan Chen, Yingda Song. 2017. Exact simulation of the sabr model. *Operations Research (forthcoming)* .

Cai, Ning, Chenxu Li, Chao Shi. 2013. Closed-form expansions of discretely monitored Asian options in diffusion models. *Mathematics of Operations Research* **39**(3) 789–822.

Caldana, Ruggero, Gianluca Fusai. 2013. A general closed-form spread option pricing formula. *Journal of Banking & Finance* **37**(12) 4893–4906.

Caldana, Ruggero, Gianluca Fusai, Alessandro Gnoatto, Martino Grasselli. 2016. General closed-form basket option pricing bounds. *Quantitative Finance* **16**(4) 535–554.

Carmona, René, Valdo Durrleman. 2003. Pricing and hedging spread options. *Siam Review* **45**(4) 627–685.

Carmona, René, Valdo Durrleman. 2005. Generalizing the Black-Scholes formula to multivariate contingent claims. *Journal of Computational Finance* **9**(2) 43.

Carverhill, Andrew, Les Clewlow. 1990. Flexible convolution. *Risk* (April) 25–29.

Černỳ, Aleš, Ioannis Kyriakou. 2011. An improved convolution algorithm for discretely sampled Asian options. *Quantitative Finance* **11**(3) 381–389.

Curran, Michael. 1994. Valuing Asian and portfolio options by conditioning on the geometric mean price. *Management science* **40**(12) 1705–1711.

Deelstra, Griselda, Jan Liinev, Michèle Vanmaele. 2004. Pricing of arithmetic basket options by conditioning. *Insurance: Mathematics and Economics* **34**(1) 55–77.

Deelstra, Griselda, Alexandre Petkovic, Michèle Vanmaele. 2010. Pricing and hedging Asian basket spread options. *Journal of Computational and Applied Mathematics* **233**(11) 2814–2830.

Dempster, Michael Alan Howarth, SS George Hong. 2002. Spread option valuation and the fast fourier transform. *Mathematical Finance–Bachelier Congress 2000*. Springer, 203–220.

Fusai, Gianluca, Daniele Marazzina, Marina Marena. 2011. Pricing discretely monitored Asian options by maturity randomization. *SIAM Journal on Financial Mathematics* **2**(1) 383–403.

Fusai, Gianluca, Attilio Meucci. 2008. Pricing discretely monitored Asian options under Lévy processes. *Journal of Banking & Finance* **32**(10) 2076–2088.

Geman, Hélyette, Marc Yor. 1993. Bessel processes, Asian options, and perpetuities. *Mathematical Finance* **3**(4) 349–375.

Gentle, David. 1993. Basket weaving. *Risk* (June) 51–52.

Hagan, Patrick S, Deep Kumar, Andrew S Lesniewski, Diana E Woodward. 2002. Managing smile risk. *Wilmott* (September) 84–108.

Heston, Steven L. 1993. A closed-form solution for options with stochastic volatility with applications to bond and currency options. *Review of financial studies* **6**(2) 327–343.

Hull, John, Alan White. 1987. The pricing of options on assets with stochastic volatilities. *The journal of finance* **42**(2) 281–300.

Hurd, Thomas R, Zhuowei Zhou. 2010. A Fourier transform method for spread option pricing. *SIAM Journal on Financial Mathematics* **1**(1) 142–157.

Ju, Nengjiu. 2002. Pricing Asian and basket options via Taylor expansion. *Journal of Computational Finance* **5**(3) 79.

Kemna, Angelien GZ, ACF Vorst. 1990. A pricing method for options based on average asset values. *Journal of Banking & Finance* **14**(1) 113–129.

Kirk, Ewan. 1995. Correlation in the energy markets. *Managing energy price risk*, 1st ed. Risk Publications London, 71–78.

Krekel, Martin, Johan de Kock, Ralf Korn, Tin-Kwai Man. 2004. An analysis of pricing methods for basket options. *Wilmott Magazine* (July) 82–89.

Leentvaar, CCW, Cornelis W Oosterlee. 2008. Multi-asset option pricing using a parallel Fourier-based technique. *Journal of Computational Finance* **12**(1) 1–26.

Levy, Edmond. 1992. Pricing European average rate currency options. *Journal of International Money and Finance* **11**(5) 474–491.

Levy, Edmond, Stuart Turnbull. 1992. Average intelligence. *Risk* (Feb) 53–57.

Li, Minqiang, Shi-jie Deng, Jieyun Zhou. 2008. Closed-form approximations for spread option prices and greeks. *The Journal of Derivatives* **15**(3) 58–80.

Linetsky, Vadim. 2004. Spectral expansions for Asian (average price) options. *Operations Research* **52**(6) 856–867.

Lo, Chi-Fai. 2015. Pricing spread options by the operator splitting method. *Wilmott* (September) 64–67.

Margrabe, William. 1978. The value of an option to exchange one asset for another. *The journal of finance* **33**(1) 177–186.

Milevsky, Moshe Arye, Steven E Posner. 1998a. Asian options, the sum of lognormals, and the reciprocal gamma distribution. *Journal of financial and quantitative analysis* **33**(03) 409–422.

Milevsky, Moshe Arye, Steven E Posner. 1998b. A closed-form approximation for valuing basket options. *The Journal of Derivatives* **5**(4) 54–61.

Pearson, Neil D. 1995. An efficient approach for pricing spread options. *The Journal of Derivatives* **3**(1) 76–91.

Posner, Steven E, Moshe A Milevsky. 1998. Valuing exotic options by approximating the SPD with higher moments. *The Journal of Financial Engineering* **7**(2).

Ravindran, Kanoo. 1993. Low-fat spreads. *Risk* (Oct) 56–57.

Rogers, L Chris G, Zo Shi. 1995. The value of an Asian option. *Journal of Applied Probability* 1077–1088.

Turnbull, Stuart M, Lee Macdonald Wakeman. 1991. A quick algorithm for pricing European average options. *Journal of financial and quantitative analysis* **26**(03) 377–389.

Willard, Gregory A. 1997. Calculating prices and sensitivities for path-independent derivatives securities in multifactor models. *The Journal of Derivatives* **5**(1) 45–61.

Yor, Marc. 1992. On some exponential functionals of brownian motion. *Advances in Applied Probability* 509–531.

Zhang, Bowen, Cornelis W Oosterlee. 2013. Efficient pricing of European-style Asian options under exponential Lévy processes based on Fourier cosine expansions. *SIAM Journal on Financial Mathematics* **4**(1) 399–426.

Zhou, Jinke, Xiaolu Wang. 2008. Accurate closed-form approximation for pricing Asian and basket options. *Applied Stochastic Models in Business and Industry* **24**(4) 343–358.